E3S Web of Conferences 716, 04038 (2026) https://doi.org/10.1051/e3sconf/202671604038
IAQVEC 2026

Urban energy–microclimate digital twin: census-tract validation using mobile traverses and utility billing benchmarking

Soroush Samareh Abolhassani[1,*], *Alimohammad* Sedaghat[1], *Mojtaba* Parsaee[2,3], *David* J. Sailor[1], and *Sami* G. Al-Ghamdi[4]

[1]School of Geographical Sciences and Urban Planning, Arizona State University, Tempe, AZ, USA
[2]School of Architecture, Mississippi State University, Mississippi State, MS, USA
[3]Data Science Academic Institute, Mississippi State University, Mississippi State, MS, USA
[4]KAUST Climate and Livability Initiative, King Abdullah University of Science and Technology, Thuwal, Saudi Arabia

Abstract. Urban Building Energy Modeling tools increasingly couple building loads with urban microclimate, yet empirical validation in hot-arid cities remains limited. We evaluate the CityDigitalTwin (CDT) platform in a neighborhood near Arizona State University's Polytechnic Campus (Mesa, AZ) during a hot July 2025 period. CDT couples a GPU-accelerated fast-fluid-dynamics microclimate solver with an archetype-based urban building energy model, driven by boundary conditions from the nearest upwind airport weather station. Mobile vehicle traverses provide 2-m air-temperature observations for model evaluation on 19 July; neighborhood-mean absolute differences across four districts range from 0.09 to 1.30 °C (mean 0.63 °C). Electricity use for 15 single-story residential buildings is simulated using DOE/ESS-DIVE archetypes and a Min–Max Archetype Sweep over eight uncertain parameters; 87% of measured daily loads fall within the model interquartile envelope and all values lie within the simulated min–max bounds. Results indicate that CDT can reproduce both outdoor thermal patterns and cooling-dominated electricity use with accuracy suitable for neighborhood-scale planning and heat-mitigation studies.

Keywords. urban digital twin (CityDigitalTwin), urban building energy modeling (UBEM), urban microclimate modeling, utility-billing benchmarking, hot-arid cities

1 Introduction

Rapid urban growth and densification are changing city microclimates, increasing heat stress and building energy demand. The built environment is a major driver of the Urban Heat Island (UHI) effect and accounts for about 39% of annual global greenhouse gas (GHG) emissions [1, 2]. Around 80% of building life-cycle energy use occurs during operation, so buildings are central to decarbonization targets, including the U.S. goal of net-zero emissions by 2045 [3].

Urban Building Energy Modeling (UBEM) has become an important tool to study these issues. UBEM develops bottom-up, engineering-based models of building energy use for districts and entire cities, using inputs such as building geometry, physical properties, weather, and internal gains [4, 5]. As an upscaling of conventional BEM, it faces specific challenges, including collecting detailed urban-scale data, defining representative archetypes, and balancing model detail with computational cost. When these challenges are addressed, UBEM can support planners, policymakers, and utilities in design, policy evaluation, and energy-demand forecasting.

Urban microclimate strongly affects building energy performance, and a key challenge for bottom-up UBEM is coupling it with urban microclimate models to capture two-way interactions between buildings and the urban atmosphere [6, 7]. Previously, building energy simulation and urban microclimate analysis have been treated separately. Many UBEM studies still use "typical meteorological year" (TMY) data from rural airports, which do not capture local urban conditions [8]. This approach ignores urban boundary-layer processes and can create large errors, especially during heat waves and when local airflow and anthropogenic heat are strong. Previous work shows that UBEMs use two main types of microclimate data: simulation-based and observational. Simulation-based methods generate local climate fields numerically but are computationally demanding and require non-trivial coupling to building energy models [9, 10]. Observational approaches use in-situ measurements and remote-sensing products, yet they require substantial resources to achieve high spatial and temporal coverage and are prone to data-quality issues such as sensor drift, communication failures, and operational problems [11].

Model validation remains a main challenge for UBEM because high-quality input data and measured energy use are often scarce, especially for capturing

*Corresponding author: ssamare1@asu.edu

spatiotemporal building energy consumption patterns. Many studies therefore validate only aggregated annual energy use; for example, Dahlström et al. [4] calibrated a regional UBEM for Gotland against energy statistics and Energy Performance Certificates (EPCs) data, achieving a 3.3% difference for single-family buildings [4]. Sherif et al. [8] used a three-step procedure at community scale, comparing archetype energy use intensities (EUIs) with handbook values, sampling mean EUI against a reference manual, and benchmarking 11 multifamily buildings, with 10 cases within a 15% error band [8]. Katal et al. [7] went further by validating both components of a coupled microclimate–energy framework: transient CityFFD microclimate fields were compared with local weather-station data, while CityBEM energy simulations were validated against measured cooling electricity, with Normalized Root Mean Square Error (NRMSE) = 22% values consistent with accepted guidelines [7]. Worthy et al. [11] show that adding earth-observational microclimate data improves test-set R^2 from about 0.55 (no climate) and 0.66 (TMY3) to 0.71, while reducing Root Mean Square Error (RMSE) by roughly 42% and 26% relative to these two baselines [11]. Overall, only a limited number of studies validate both microclimate and energy outputs within the same UBEM framework, highlighting an important gap for future research.

This study aims to address these two key gaps with two approaches: First, we use the CityDigitalTwin (CDT) tool to capture detailed urban microclimate within city-scale building energy modelling. Second, we provide validation of both microclimate and building energy use, using car-based field measurements and fixed weather stations, and benchmarking building electricity consumption against data from 15 buildings from SRP in the Phoenix area.

2 Methodology

This study validates CDT coupled energy-microclimate simulation in Mesa, Arizona during summer 2025 (July). Both domains are assessed within the same neighborhood near Arizona State University's Polytechnic Campus: microclimate predictions are validated using vehicle-based mobile traverse air temperature measurements, while building energy simulations are benchmarked against utility-billing data from 15 residential buildings at North Desert Village. This co-located dual-domain validation addresses a critical gap in UBEM research, where microclimate and energy components are typically evaluated separately or independently.

2.1 CityDigitalTwin Platform Overview

CDT is a coupled urban-scale simulation platform developed by Planète Green Leaves that integrates microclimate modeling with building energy simulation to capture the bidirectional interactions between the built environment and local atmospheric conditions. The platform combines two core computational engines: Fast Fluid Dynamics component of CDT for microclimate simulation and Urban Building Energy Model component of CDT for building thermal and energy performance analysis. This integrated framework enables simultaneous prediction of outdoor thermal conditions and building energy consumption at city scale while maintaining computational efficiency suitable for neighborhood- and district-level applications.

2.2 Microclimate Modeling Component of CityDigitalTwin

The microclimate module employs a GPU-accelerated Fast Fluid Dynamics (FFD) solver to simulate urban aerodynamics and thermal conditions. Its semi-Lagrangian method ensures numerical stability with larger time steps and coarser resolution than traditional CFD, operating at 1-meter resolution over ~1 km² domains and requiring about 5 minutes per simulated hour on consumer-grade GPUs.

CityFFD uses Large Eddy Simulation (LES) turbulence modeling to capture urban heat-island effects and flow patterns in street canyons. It represents detailed building geometry, street layout, vegetation, and boundary conditions such as terrain, soil temperature, and coupled surface temperatures. The CUDA-based architecture enables efficient processing of millions of cells, supporting routine urban-planning applications.

2.3 Building Energy Modeling Component of CityDigitalTwin

The building energy module performs minute-level single-zone thermal simulations. Each building is modeled as a well-mixed air volume with loads from convection, infiltration, and internal gains. A one-dimensional resistance capacitance (RC) network computes transient heat conduction through envelope surfaces.

Window heat transfer is solved using glazing heat-balance equations, with solar gains derived from Solar Heat Gain Coefficient (SHGC) and incident radiation. HVAC systems follow Coefficient of Performance (CoP) curves and thermostat setpoints. Computation requires roughly 2 minutes per simulated hour per building, enabling district-scale modeling.

Building thermal properties come from DOE/NREL archetypes that describe envelope specifications, internal loads, occupancy schedules, and HVAC systems. For Phoenix, archetypes were sourced from the DOE ESS-DIVE database [12] to reflect the Southwestern U.S. building stock.

2.4 Mobile Traverse Measurement Protocol

Air temperature measurements were collected using a vehicle-based traverse method to generate high-resolution validation data for subsequent microclimate simulations. Air temperature was recorded at approximately 2 m above ground level while the vehicle followed predetermined routes across the North Desert Village in Mesa, Arizona area (see Figure 1).

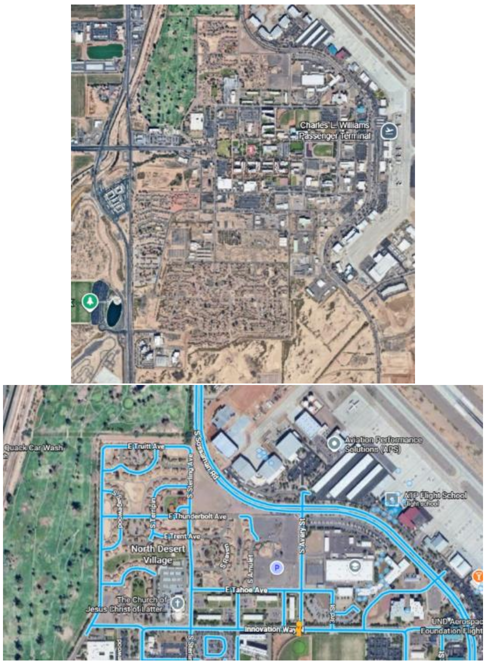

Fig. 1. Vehicle traverse route for mobile air-temperature measurements near ASU's North Desert Village in Mesa, Arizona.

A vehicle was equipped with three instruments (Figure 2): (i) a window-mounted resistance temperature detector (RTD) with an onboard logger for ambient air temperature, (ii) a side-mounted infrared (IR) surface temperature sensor positioned approximately 25–30 cm above ground level and angled toward the road centerline, and (iii) a GPS data logger hung from the rear-view mirror to record vehicle location and synchronize with temperature data streams. Sensors were pre-programmed for continuous logging, and all devices were powered by internal batteries with sufficient storage capacity for multiple traverses.

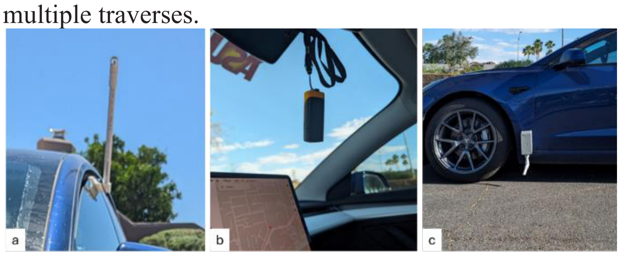

Fig. 2. Instrumentation setup for vehicle-based traverse measurements in Phoenix. (a) Window-mounted resistance temperature detector (RTD) used for ambient air temperature measurements. (b) GPS logger suspended from the rear-view mirror to record geolocation. (c) Infrared (IR) surface temperature sensor mounted 25–30 cm above ground on the driver's side of the vehicle, angled toward the street centerline.

The traverse measurement lasted approximately 15 minutes, conducted at a vehicle speed of 2–4 m/s across the district. Raw data were downloaded daily and merged using GPS timestamps. Air and surface temperature records were georeferenced to produce spatially continuous fields. These datasets serve both as empirical evidence of Phoenix's thermal landscape and as calibration/validation inputs for the microclimate model presented in the next section.

2.5 Building Energy Model Validation: Utility-Billing Benchmarking

To validate the building energy modeling component of CDT, a case study was conducted in a neighborhood in Mesa, Arizona, covering 804 buildings (Figure 3). Within this area, a smaller neighborhood, North Desert Village, part of the Arizona State University (ASU) campus, was selected for measured data collection. This neighborhood comprises single-story residential student housing units. Fifteen buildings were prioritized for validation and calibration based on their similar architectural characteristics, including tan-colored roofs, nominal north–south orientation, and the absence of roof modifications. These buildings, whose total electricity consumption data were available for validation, are highlighted with blue circles in Figure 3. The electricity consumption data were obtained from the Salt River Project (SRP), the local utility serving the Mesa metropolitan area.

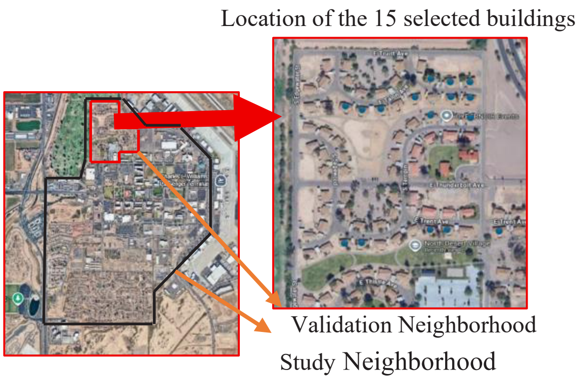

Fig. 3. Aerial view of the selected neighborhood in North Desert Village, Arizona State University campus. The highlighted area includes the 15 single-story residential buildings (tan roofs, nominally N–S orientation) used in the UBEM case study.

The CDT archetype inputs, envelope properties, and occupancy schedules were extracted from the U.S. Department of Energy (DOE) residential building stock archetypes hosted on the Environmental Systems Science Data Infrastructure for a Virtual Ecosystem (ESS-DIVE) repository. This dataset was developed by Oak Ridge National Laboratory (ORNL) as part of DOE's residential energy use characterization efforts. It provides standardized archetypes for U.S. building stock, including construction-era-specific data on geometry, thermal envelope properties, internal loads, and operational schedules, which are widely used in UBEM studies. Model validation was conducted by comparing simulated energy results with actual electricity consumption data for the 15 selected buildings during July 2025.

Model performance was evaluated against ASHRAE Guideline 14 criteria, which specify maximum thresholds of 15% for Coefficient of Variation of Root Mean Square Error (CV(RMSE)) and ±5% for Normalized Mean Bias Error (NMBE) when using monthly calibration data.

Calibration employed a Min-Max Archetype Sweep (MMAS) methodology, systematically exploring 256 parameter combinations (2^8) derived from literature-based ranges. Eight key parameters were varied between documented minimum and maximum values: occupancy density (0.015-0.025 people/m²), equipment power density (4.0-8.0 W/m²), lighting power density (5.0-9.0 W/m²), infiltration rate (0.3-0.7 ACH), cooling setpoint (23-26°C), heating setpoint (19-22°C), HVAC cooling COP (2.5-3.5), and heating efficiency (75-90%). Parameter ranges were established from DOE ResStock documentation [13], ASHRAE Standard 90.1 [14], and Building America research programs [15]. The resulting simulation ensemble generates daily distributions of energy consumption across all parameter combinations, creating physically plausible performance bounds for comparison with measured data.

3 Results and discussions

3.1 Spatial Temperature Patterns from Mobile Traverse Measurements

Figure 4 presents air temperature measurements collected via mobile traverse in the vicinity of Arizona State University's Polytechnic Campus in southeast Mesa, Arizona, during peak afternoon conditions on July 19, 2025. The traverse covered approximately 8 km of residential and institutional streets between 1:14 PM and 1:30 PM, with temperature readings recorded every 2 seconds using a DwyerOmega Class A RTD sensor mounted to the vehicle's driver-side window and housed in a radiation-shielded PVC enclosure to minimize solar heating artifacts.

The spatial temperature distribution reveals microscale thermal heterogeneity across the study domain, with observed air temperatures ranging from approximately 38°C to 40°C. This 2°C temperature gradient within the confined urban area demonstrates the influence of local surface properties, building morphology, and vegetation cover on near-surface air temperature under summer desert conditions. The traverse route encompasses diverse land use contexts, including residential neighborhoods with varying tree canopy cover, ASU campus facilities with mixed building heights and open spaces, and arterial corridors with impervious surfaces.

Several spatial patterns emerge from the temperature field. Cooler zones (38-38.5°C, represented by purple coloration) correspond predominantly to areas with established tree canopy and residential streets with moderate building density, where afternoon shading from structures and vegetation reduces solar heat absorption by ground surfaces. The warmest measurements (39.5-40°C, orange-red zones) appear concentrated along the eastern portion of the traverse route, particularly near major roadways and the athletic field area with extensive exposed surfaces and limited vegetation, consistent with established urban heat island mechanisms in hot-arid environments.

The short data-collection window (16 minutes) ensures that measured temperature differences reflect true spatial variation rather than changes in solar angle or atmospheric conditions. The high sampling frequency (2-second intervals, ~480 points) provides sufficient spatial resolution to capture temperature changes across land-cover boundaries and between streets. Notable thermal features include the relatively cooler western residential areas (purple segments) compared to the warmer eastern campus core and athletic facilities (orange segments). The traverse path exhibits distinct thermal zones: the northwestern residential loop shows sustained cooler temperatures (38-38.5°C), while the southeastern portion near open athletic fields registers peak warming (39.5-40°C). This east-west thermal gradient of approximately 2°C across less than 1 kilometer demonstrates the rapid spatial variability of urban air temperature under intense solar loading conditions.

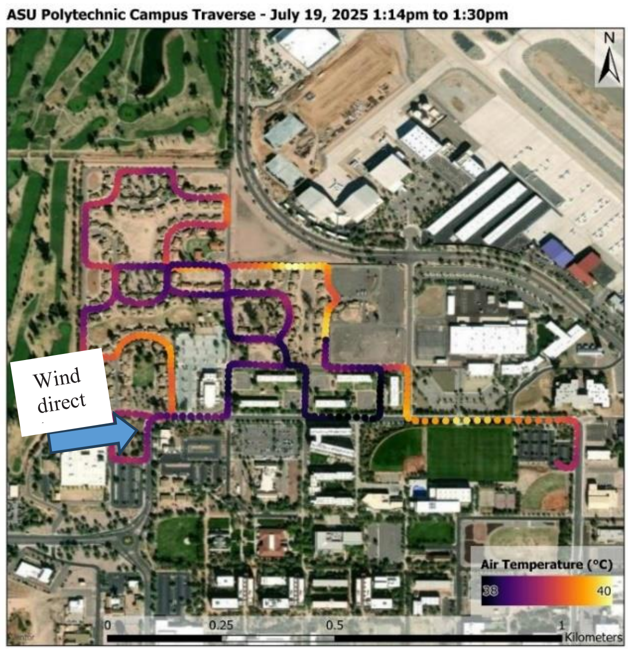

Fig. 4. Car based air temperature traverse near the ASU Polytechnic Campus in southeast Mesa, Arizona. Data collected every 2 seconds with a DwyerOmega Class A RTD temperature sensor housed in a PVC shield and mounted to the driver's side window. Collection window between the 1:14pm and 1:30pm on July 19, 2025 (wind direction: 265; wind speed: 2.51).

These empirical temperature fields serve dual purposes in the validation framework: first, they provide ground-truth observations of actual thermal conditions experienced at pedestrian and vehicular level during summer afternoons in Phoenix, capturing spatial variability that fixed weather stations cannot resolve; second, they enable direct comparison with CDT microclimate simulation outputs through spatial interpolation and statistical metrics (RMSE, MAE, spatial correlation) described in the validation methodology. The observed 2°C temperature range across the relatively compact study domain underscores the importance of incorporating high-resolution microclimate modeling in urban building energy assessments, as conventional approaches using single-station weather data would fail to capture these spatial gradients that directly influence building cooling loads in hot desert cities.

3.2 Building Energy Validation Results and MMAS Calibration

Figure 5 illustrates energy consumption (kWh) for 804 buildings simulated. Buildings are color-coded according to their total energy demand for July 2025, ranging from 184 to 654,994 kWh, as indicated by the legend. High-consumption zones (red and orange) correspond primarily to large institutional, commercial, hospital, and research facilities, whereas low-consumption zones (green) represent single-story residential buildings, including those in South Desert Village. This wide range occurs because the map includes both very large, high-intensity buildings with long operating hours and heavy cooling loads, and much smaller, low-intensity homes that are used only part of the day. The left-panel statistics summarize the building count, energy range, and categorical energy levels used in the simulation.

Fig. 5. Spatial distribution of simulated building energy consumption across 804 buildings in Mesa, Arizona for July 2025.

The UBEM validation was conducted using measured electricity consumption data from 15 single-story residential buildings at Arizona State University's North Desert Village during July 2025. Model performance was evaluated against ASHRAE Guideline 14 criteria, which specify maximum thresholds of 15% for CV(RMSE) and ±5% for NMBE when using monthly calibration data.

Figure 6 presents the daily energy consumption distribution and corresponding outdoor temperature conditions for the 15-building validation subset during July 2025, illustrating the Min-Max Archetype Sweep (MMAS) calibration methodology. The top panel displays the measured electricity consumption data (red line) overlaid on simulation envelopes generated from 256 parameter combinations (green boxplots), where each boxplot represents the distribution of daily average energy consumption across all tested parameter combinations for a given day. The bottom panel shows outdoor dry bulb temperature variations throughout the month, with daily mean temperatures (dark red line) overlaid on hourly temperature distributions (orange boxplots), providing critical context for understanding building energy performance under varying thermal loads.

The MMAS calibration approach systematically explored the parameter space by testing all combinations of minimum and maximum values for 8 key building parameters (2^8 = 256 combinations), drawn from literature-based ranges established by DOE Residential Building Stock documentation, ASHRAE standards, and Building America research programs (see Table 1). Similar ranges for occupancy density, internal loads, infiltration, and thermostat setpoints have been adopted in large-scale residential stock models and protocols, including the ResStock technical reference documentation and the Building America House Simulation Protocols, as well as in high-granularity stock modeling studies (e.g., [13, 16, 17])

Table 1. MMAS calibration parameters with literature-based minimum and maximum values from DOE ResStock, ASHRAE, and Building America standards.

Parameter	Unit	MIN Value	MAX Value	Source
Occupancy Density	people /m²	0.015	0.025	DOE ResStock [14]
Equipment Power Density	W/m²	4.0	8.0	ASHRAE 90.1 [18]
Lighting Power Density	W/m²	5.0	9.0	ASHRAE 90.1 [18]
Infiltration Rate	ACH	0.3	0.7	Building America [15]
Cooling Setpoint	°C	23	26	DOE ResStock [14]
Heating Setpoint	°C	19	22	DOE ResStock [14]
HVAC COP (Cooling)	-	2.5	3.5	ASHRAE [19]
HVAC Efficiency (Heating)	%	75	90	ASHRAE [19]

These parameters included occupancy density, internal load intensities (equipment and lighting power densities), infiltration rates, temperature setpoints (cooling and heating), and HVAC system performance (cooling COP and heating efficiency). The resulting simulation ensemble creates upper and lower bounds (whiskers) and interquartile ranges (boxes) that establish the physically plausible performance envelope for the residential building stock.

The measured consumption data (red line, top panel) demonstrates strong temporal correlation with the simulation envelope throughout the month. During the first week (Days July 1-7, 2025), measured consumption ranged from 30-43 kWh/hour and fell consistently within or near the interquartile range of simulated values, indicating well-calibrated model parameters. A notable consumption drop occurred around Day 20 (23 kWh/hour), representing expected physical behavior that the simulation ensemble successfully captured through its lower bounds. Similarly, at the end of the month (Day 31), both measured consumption and outdoor temperatures decreased significantly (dropping from ~39°C to ~30°C), further demonstrating the model's ability to capture climate-driven load variations.

The temperature distribution (bottom panel) reveals typical Phoenix summer conditions with daily mean temperatures ranging from 30°C to 40°C throughout most of July. Hourly temperature variations show diurnal swings of 10-15°C, with peak afternoon temperatures reaching 43-46°C during mid-month and minimum nighttime temperatures around 25-28°C. The sustained high temperatures during Days 11-17 directly correspond to peak energy consumption periods in the top panel, demonstrating the strong coupling between outdoor thermal conditions and building cooling loads in this desert climate.

The simulation envelope exhibits systematic patterns consistent with Phoenix's cooling-dominated climate. Peak consumption predictions occurred during mid-month (Days 11-17), with maximum bounds reaching 54-56 kWh/hour, corresponding to periods of sustained high outdoor temperatures (38-40°C mean daily) and elevated cooling demand. The boxplot distributions show relatively tight interquartile ranges (typically 8-12 kWh/hour spread) during stable weather conditions, indicating parameter convergence for typical operating conditions. Wider distributions during peak and off-peak periods reflect increased parameter sensitivity under extreme thermal loads.

Critical to the MMAS methodology, the MIN and MAX simulation bounds were properly identified based on actual simulation performance rather than parameter combinations. The minimum bound (whisker bottom) represents the parameter combination producing the lowest daily average consumption across all 256 runs, while the maximum bound (whisker top) represents the highest-consuming combination. This approach ensures that the envelope boundaries reflect true performance extremes rather than arbitrary parameter settings, providing physically meaningful confidence intervals for energy predictions.

The dual-panel visualization reveals several important validation insights. First, approximately 87% of measured daily values (27 of 31 days) fall within the simulation interquartile range (Q1-Q3), indicating strong central tendency agreement between model and measurements. Second, all measured values remain within the min-max whisker bounds, confirming that the literature-based parameter ranges encompass actual building performance. Third, the temporal pattern of measured consumption closely tracks both the simulation median and outdoor temperature variations, demonstrating that the model captures both absolute magnitudes and dynamic thermal responses to changing environmental conditions. The correlation between temperature patterns and energy consumption validates the physical realism of the simulation framework and confirms appropriate representation of climate-driven cooling loads in Phoenix's desert environment.

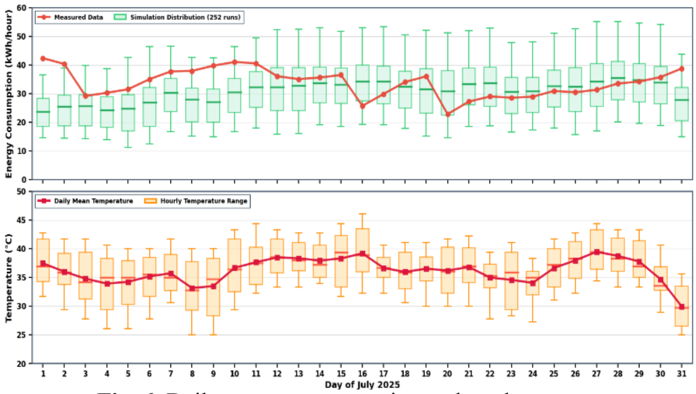

Fig. 6. Daily energy consumption and outdoor temperature distributions during July 2025 validation (15 buildings). Measured consumption (red line) overlaid on simulation envelopes from 256 MMAS parameter combinations (green boxplots: Q1-Q3; whiskers: min-max). Bottom panel shows outdoor temperature patterns (orange boxplots: hourly range; dark red line: daily mean).

3.3 Microclimate Validation Results and Calibration Performance

Figure 7 shows the simulated near-surface air temperature field from CDT at 13:00 on 19 July 2025, corresponding to the mobile-traverse campaign described earlier. Four subdistricts within the main validation area were selected to represent distinct morphological and land-use contexts: two predominantly low-rise residential neighborhoods (D1, D3) and two mixed or institutional blocks with larger buildings and more open paved areas (D2, D4). For each district, all traverse measurements falling inside the outlined polygon were averaged and compared with the spatial mean of CDT 2 m air temperature over the same area at 13:00. This aggregation minimizes representativeness errors from slight mismatches in vehicle position and grid cell centroids while emphasizing neighborhood-scale thermal performance rather than point-by-point noise.

The resulting absolute differences between observed and simulated mean air temperatures are 0.84, 0.27, 1.30, and 0.09 °C for districts D1–D4, respectively (Table 2).

Table 2. Neighborhood-scale microclimate validation statistics at 13:00 on 19 July 2025. Absolute difference is computed as |T_sim – T_obs| for area-averaged 2 m air temperature.

District	|T_sim – T_obs| (°C)
D1	0.84
D2	0.27
D3	1.30
D4	0.09
Mean	**0.63**

The spread across districts is modest (population standard deviation ≈ 0.48 °C), and three of the four neighborhoods exhibit errors below 1 °C. Averaged over all districts, CDT under/over predicts neighborhood mean air temperature by only 0.63 °C, corresponding to a normalized error of about 1.6% relative to the 38 °C background temperature measured at the reference airport station. From a calibration standpoint, these biases are comparable to or smaller than uncertainties associated with sensor accuracy, unresolved vegetation shading, and short-term variability during the 16 min traverse window. The largest discrepancy occurs in D3, one of the low-rise residential neighborhoods, suggesting that further refinement of tree canopy representation and surface material properties in this area could yield additional improvements. Nevertheless, the overall pattern of warmer open corridors and cooler, vegetation-rich neighborhoods evident in the measurements is reproduced by CDT, and the magnitude of modeled temperature contrasts between the four districts closely matches the observations.

All microclimate simulations were forced using boundary conditions from the nearest upwind airport station located outside the urban core at 13:00 on 19 July 2025. These data provide the background temperature, humidity, radiation, wind, and solar-geometry inputs for CDT; the main variables are summarized in Table 3.

Table 3. Weather boundary conditions used to drive CDT microclimate simulation at 13:00 on 19 July 2025 (nearest upwind airport station).

Variable (column)	Value	Unit	Description
Date / time	19(Jul 2025, 13:00	–	Local time of simulation and traverse
Air temperature (outTemDrb)	38	°C	Dry-bulb air temperature
Dew-point temperature (outTemDep)	8.1	°C	Dew-point temperature
Relative humidity (outRH)	15.0	%	Ambient relative humidity
Global horizontal irradiance (outTSolHr)	946	W/m²	Total solar on horizontal surface
Diffuse horizontal irradiance (outSolDHI)	158	W/m²	Diffuse horizontal solar irradiance
Direct normal irradiance (outSolDNI)	809.4	W/m²	Direct normal solar irradiance
Wind speed (outWindS)	2.51	m/s	10-m wind speed
Wind direction (outWindD)	265.0	°	Meteorological direction (from which wind blows)
Solar zenith angle (outSolZe)	14.01	°	Solar zenith angle
Cosine of solar zenith (outSolCZe)	0.95	–	cos(zenith angle)
Solar azimuth from south (outSolAzS)	27.21	°	Solar azimuth measured from south
Solar azimuth from north (outSolAzN)	207.21	°	Solar azimuth measured from north

The selection of the upwind airport station as the sole boundary-condition source warrants discussion because CDT inherits any bias present in that reference. Informal sensitivity tests in which the boundary dry-bulb temperature was perturbed by ±1 °C shifted district-mean air-temperature predictions by a comparable magnitude, confirming that accurate upstream observations are critical to simulation fidelity. The present choice balances data quality, regulatory traceability, and proximity to the study domain; however, reliance on a single point source means that mesoscale heterogeneity in the background flow is not captured. Future implementations could incorporate multi-station blending or mesoscale-model downscaling to reduce boundary-condition sensitivity, particularly when extending CDT to larger urban domains where a single reference station may not adequately represent the upstream atmospheric state.

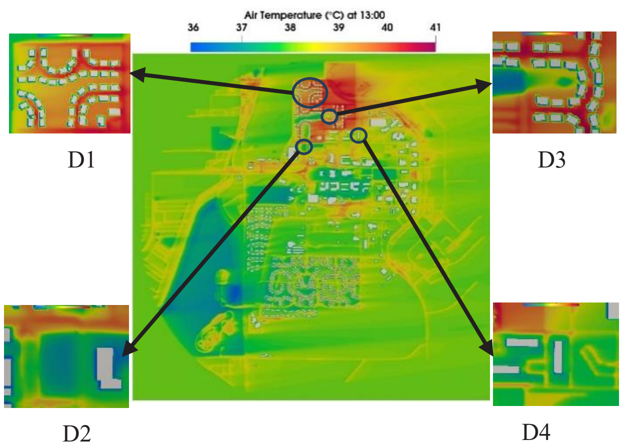

Fig. 7. Simulated 2 m air temperature at 13:00 on 19 July 2025, with inset panels highlighting the four neighborhood districts (D1–D4) used for microclimate validation against mobile traverse measurements.

4 Conclusion

CDT was validated in Mesa, Arizona, using July 2025 utility billing data from 15 residential buildings together with mobile traverse microclimate measurements. The Min–Max Archetype Sweep calibration produced a simulation envelope that enclosed all measured daily electricity use, while neighborhood scale microclimate validation across four districts yielded mean absolute temperature differences between 0.09 and 1.30 °C (overall mean 0.63 °C). These results indicate that CDT can reliably reproduce both building energy use and outdoor thermal patterns, supporting its application to planning and heat mitigation studies in hot desert cities.

Several avenues for future development can further strengthen the CDT framework. Extending the platform to larger urban domains will require strategies such as domain decomposition and multi-GPU parallelization to maintain 1-m resolution while scaling beyond the present ~1 km² neighborhood. Adopting multi-station blending or mesoscale-model downscaling would reduce sensitivity to a single upstream reference station. Additional validation under diverse climatic contexts, building typologies, and seasonal conditions will also be necessary to establish the generalizability of the coupled microclimate–energy modeling approach.

References

1. United Nations Environment Programme, 2023 Global Status Report for Buildings and Construction: Beyond Foundations – Mainstreaming Sustainable Solutions to Cut Emissions from the Buildings Sector (United Nations Environment Programme, 2024), https://doi.org/10.59117/20.500.11822/45095
2. International Energy Agency, International Renewable Energy Agency, United Nations Climate Change, The Breakthrough Agenda Report 2022: Accelerating Sector Transitions Through Stronger International Collaboration (OECD, 2022), https://doi.org/10.1787/692cdb6b-en
3. K.I. Praseeda, B.V. Venkatarama Reddy, M. Mani, Life-Cycle Energy Assessment in Buildings: Framework, Approaches, and Case Studies, in Encyclopedia of Sustainable Technologies (Elsevier, 2017), https://doi.org/10.1016/B978-0-12-409548-9.10188-5
4. L. Dahlström, F. Johari, J. Widén, Energy Build. 346, 116178 (2025), https://doi.org/10.1016/j.enbuild.2025.116178
5. D. Kong, A. Cheshmehzangi, Z. Zhang, S. Pourroostaei Ardakani, T. Gu, Energy Effic. 16, 69 (2023), https://doi.org/10.1007/s12053-023-10147-z
6. T. Hong, Y. Chen, X. Luo, N. Luo, S.H. Lee, Build. Environ. 168, 106508 (2020), https://doi.org/10.1016/j.buildenv.2019.106508
7. A. Katal, M. Mortezazadeh, L. Wang, H. Yu, Energy 251, 123817 (2022), https://doi.org/10.1016/j.energy.2022.123817
8. T. Sherif, R. Katia, M. Nguyen, N. Ma, T. Rakha, Appl. Energy 383, 125342 (2025), https://doi.org/10.1016/j.apenergy.2025.125342
9. N. Sezer, H. Yoonus, D. Zhan, L. Wang, I. Galal Hassan, M. Azizur Rahman, Renew. Sustain. Energy Rev. 184, 113577 (2023), https://doi.org/10.1016/j.rser.2023.113577
10. N. Abbasabadi, M. Ashayeri, Build. Environ. 161, 106270 (2019), https://doi.org/10.1016/j.buildenv.2019.106270
11. A. Worthy, M. Ashayeri, N. Abbasabadi, Sustain. Cities Soc. 130, 106544 (2025), https://doi.org/10.1016/j.scs.2025.106544
12. Environmental Systems Science Data Infrastructure for a Virtual Ecosystem (ESS-DIVE), U.S. Department of Energy, Lawrence Berkeley National Laboratory, https://data.ess-dive.lbl.gov/view/doi%3A10.15485%2F2212792 (accessed 31 October 2025)
13. J. Reyna, A. Fontanini, E. Present, L. Liu, R. Adhikari, C. Bianchi, et al., ResStock Technical Reference Documentation v3.3.0, NREL/TP-5500-91621 (National Renewable Energy Laboratory, Golden, CO, 2025)
14. ASHRAE, ANSI/ASHRAE/IES Standard 90.1-2019: Energy Standard for Buildings Except Low-Rise Residential Buildings (American Society of Heating, Refrigerating and Air-Conditioning Engineers, Atlanta, GA, 2019)
15. R. Hendron, C. Engebrecht, Building America House Simulation Protocols, NREL/TP-550-49246 (National Renewable Energy Laboratory, Golden, CO, 2010), https://www.nrel.gov/docs/fy11osti/49246.pdf
16. E. Wilson, C. Engebrecht Metzger, S. Horowitz, R. Hendron, 2014 Building America House Simulation Protocols, NREL/TP-5500-60988 (National Renewable Energy Laboratory, Golden, CO, 2014)
17. E. Wilson, C. Christensen, S. Horowitz, H. Horsey, A High Granularity Approach to Modeling Energy Consumption and Savings Potential in the U.S. Residential Building Stock, in Proceedings of the ASHRAE and IBPSA USA SimBuild 2016 Building Performance Modeling Conference 6, 396–406 (2016)
18. ASHRAE, 2024 ASHRAE Handbook – HVAC Systems and Equipment (American Society of Heating, Refrigerating and Air-Conditioning Engineers, Atlanta, GA, 2024)
19. E.J.H. Wilson, C. Christensen, S. Horowitz, J. Robertson, J. Maguire, Energy Efficiency Potential in the U.S. Single-Family Housing Stock, NREL/TP-5500-68670 (National Renewable Energy Laboratory, Golden, CO, 2017), https://docs.nrel.gov/docs/fy18osti/68670.pdf